

# Assembly of Organic–Inorganic Hybrid Materials Based on Dawson-Type Polyoxometalate and Multinuclear Copper–Phen Complexes with Unique Magnetic Properties

Chun-Dan Zhang, Shu-Xia Liu,\* Chun-Yan Sun, Feng-Ji Ma, and Zhong-Min Su\*

Key Laboratory of Polyoxometalate Science of Ministry of Education, College of Chemistry, Northeast Normal University, Changchun, Jilin 130024, China

Received April 7, 2009; Revised Manuscript Received June 15, 2009

**ABSTRACT:** Two novel hybrid compounds,  $[\text{Cu}_2(\text{Phen})_4\text{Cl}][\text{Cu}_2(\text{Phen})_3(\text{H}_2\text{O})\text{Cl}][\text{P}_2\text{W}_{18}\text{O}_{62}] \cdot \text{H}_2\text{O}$  (**1**) and  $[\text{Cu}_7(\text{Phen})_7(\text{H}_2\text{O})_4\text{Cl}_8][\text{P}_2\text{W}_{18}\text{O}_{62}] \cdot 6\text{H}_2\text{O}$  (**2**) (Phen = 1,10-phenanthroline), containing multinuclear  $\text{Cu}^{\text{II}}$  complex cations, have been obtained in hydrothermal conditions and characterized by IR, elemental, thermogravimetric, magnetic, electrochemical and single-crystal X-ray diffraction analyses. The main structural feature to these two compounds is the presence of different copper–Phen complex moieties which compose new multinuclear copper–Phen complexes linked by a Cu–Cl bond. The binuclear cations  $[\text{Cu}_2(\text{Phen})_4\text{Cl}]^{3+}$  and  $[\text{Cu}_2(\text{Phen})_3(\text{H}_2\text{O})\text{Cl}]^{3+}$  of **1** indicate a special chiral arrangement. The **2** contains a heptanuclear copper chain  $[\text{Cu}_7(\text{phen})_7(\text{H}_2\text{O})_4\text{Cl}_8]^{6+}$  formed by a one-Cl bridge and a two-Cl bridge. Magnetic studies prove that Cu–Cl–Cu angles result in different magnetic behaviors in **1** and **2**. Furthermore, a compound **2**-modified carbon paste electrode (**2**-CPE) displays good electrocatalytic activity toward the reduction of nitrite.

## Introductions

The POM-based hybrids have emerged as a major research area for the rational design of new materials due to their intriguing topological structures and their widespread applications.<sup>1</sup> They have been significantly enriched by the introduction of transition metal complexes (TMCs) which can employ the polydentate ligands to stabilize or bridge the metal ions and form multinuclear spin clusters with unique properties.<sup>2–4</sup> The interest of supporting TMCs, which have been extensively studied in magnetostructural research areas, on POMs lies in the possibility of tuning the magnetic properties due to their high dependence on the nature and spatial disposition of the ligands.

In recent years, attention has been mainly focused on the copper(II) complexes of Phen ligand due to their variable nuclearities and magnetic properties.<sup>5,6</sup> Some hybrid compounds are assembled by polyoxoanions and different copper–Phen complexes with nuclearities ranging from one to four, but the bridging ligands are usually limited in carboxylate species (such as acetate and oxalate).<sup>7,8</sup> And these compounds usually indicate antiferromagnetic coupling because a carboxylate bridging ligand can mediate magnetic exchange interactions between metal ions.

Currently, we are exploring the design and development of new hybrid materials containing copper–Phen complexes and POMs by changing bridging ligands, and we expect that novel compounds with high nuclear magnetic clusters can be obtained and studied in magnetostructural research work. During this ongoing effort, Cl is the preferred bridging ligand because the architectures of compounds with a Cl bridge can be tuned at the molecular level so as to possess interesting topological structure, various components and potential applications in the area of magnetism.<sup>9,10</sup> Because their mixing usually results in precipitation, making it difficult to grow crystals of complexes, we adopted a hydrothermal technique and successfully synthesized two novel complexes,  $[\text{Cu}_2(\text{Phen})_4\text{Cl}][\text{Cu}_2(\text{Phen})_3-$

$(\text{H}_2\text{O})\text{Cl}][\text{P}_2\text{W}_{18}\text{O}_{62}] \cdot \text{H}_2\text{O}$  (**1**) and  $[\text{Cu}_7(\text{Phen})_7(\text{H}_2\text{O})_4\text{Cl}_8]-[\text{P}_2\text{W}_{18}\text{O}_{62}] \cdot 6\text{H}_2\text{O}$  (**2**). Herein, the syntheses, structures, magnetic and electrochemical properties of compounds **1** and **2** have been reported. They display different magnetic behaviors because different Cl bridges result in changes of Cu–Cl–Cu angles.

## Experimental Section

**Materials and Methods.** The  $\text{Na}_{12}[\alpha\text{-P}_2\text{W}_{15}\text{O}_{56}] \cdot 18\text{H}_2\text{O}$  and  $\text{K}_{12}[\text{H}_2\text{P}_2\text{W}_{12}\text{O}_{48}] \cdot 24\text{H}_2\text{O}$  were synthesized following published procedures, and their purity was confirmed by infrared spectroscopy.<sup>11</sup> All other reagents were readily available from commercial sources and used as received without further purification. The IR spectra in KBr pellets were recorded in the range 400–4000  $\text{cm}^{-1}$  with an Alpha Centaur FT/IR spectrophotometer. Elemental analyses (C, H and N) were performed with a Perkin-Elmer 2400 CHN elemental analyzer. Cu, W, P and Cl were determined with a PLASMASPEC (I) ICP atomic emission spectrometer. Thermogravimetric analyses were carried out by using a Perkin-Elmer TGA7 instrument, with a heating rate of 10  $^\circ\text{C}/\text{min}$ , under a nitrogen atmosphere. The **2**-CPE was fabricated as follows: 1.0 g of graphite powder and 70 mg of **2** were mixed and ground together with an agate mortar and pestle to achieve a uniform and dry mixture; to the mixture 0.7 mL of paraffin oil was added and stirred with a glass rod; then the homogenized mixture was used to pack 3 mm inner diameter glass tubes. The surface was wiped with weighing paper, and electrical contact was established with a copper rod through the back of the electrode. Electrochemical measurements were performed with a CHI660B electrochemical workstation (Chenhua Instruments Co., Shanghai, China). A three-electrode system was employed in this study. A carbon paste electrode was used as a working electrode, a saturated calomel electrode (SCE) as a reference electrode, and a Pt coil as a counter electrode. All the experiments were conducted at ambient temperature ( $20 \pm 5$   $^\circ\text{C}$ ). The electron paramagnetic resonance (EPR) spectra (X-band) were recorded on a Japanese JES-FE3AX spectrometer at room temperature (290 K). Magnetic susceptibility data were collected over the temperature range 300–2 K at a magnetic field of 1000 Oe for **1** and **2** on a Quantum Design MPMS-5 SQUID magnetometer.

**Synthesis of  $[\text{Cu}_2(\text{Phen})_4\text{Cl}][\text{Cu}_2(\text{Phen})_3(\text{H}_2\text{O})\text{Cl}][\text{P}_2\text{W}_{18}\text{O}_{62}] \cdot \text{H}_2\text{O}$  (**1**).** A mixture of LiCl (0.335 g, 7.902 mmol),  $\text{CuCl}_2 \cdot 6\text{H}_2\text{O}$  (0.125 g, 0.515 mmol),  $\text{K}_{12}[\text{H}_2\text{P}_2\text{W}_{12}\text{O}_{48}] \cdot 24\text{H}_2\text{O}$  (0.25 g, 0.063 mmol), Phen (0.05 g 0.252 mmol) and  $\text{H}_2\text{O}$  (9 mL, 500 mmol) was stirred for 30 min in air until it was homogeneous, and then transferred and sealed in a 20 mL Teflon-lined stainless steel container. After being heated to 160  $^\circ\text{C}$  under autogenous pressure for 5 days, the bomb was cooled

\* Authors to whom correspondence should be addressed. Fax: +86-431-85099328. E-mail: liusx@nenu.edu.cn.

**Table 1.** Crystal Data and Structural Refinement for Compounds **1** and **2**

formula	C <sub>84</sub> H <sub>60</sub> Cl <sub>2</sub> Cu <sub>4</sub> N <sub>14</sub> O <sub>64</sub> P <sub>2</sub> W <sub>18</sub>	C <sub>84</sub> H <sub>76</sub> Cl <sub>8</sub> Cu <sub>7</sub> N <sub>14</sub> O <sub>72</sub> P <sub>2</sub> W <sub>18</sub>
formula weight (g mol <sup>-1</sup> )	5985.6	6532.9
T (K)	296(2)	296(2)
wavelength (Å)	0.71073 4	0.71073 4
crystal system	monoclinic	triclinic
space group	P2 <sub>1</sub>	P $\bar{1}$
a (Å)	14.0260(10)	14.1255(9)
b (Å)	27.3886(19)	17.2468(11)
c (Å)	16.7526(12)	28.2613(18)
V(Å <sup>3</sup> )	5934.4(4)	6653.1(7)
Z	2	2
D <sub>calc</sub> (mg m <sup>-3</sup> )	3.348	3.251
μ (mm <sup>-1</sup> )	18.234	16.862
F(000)	5364	5870
crystal size (mm)	0.25 × 0.21 × 0.18	0.25 × 0.18 × 0.15
goodness-of-fit on F <sup>2</sup>	1.021	1.003
final R indices [I > 2σ(I)] <sup>a</sup>	R <sub>1</sub> = 0.0603, wR <sub>2</sub> = 0.1424	R <sub>1</sub> = 0.0526, wR <sub>2</sub> = 0.1231
R indices (all data)	R <sub>1</sub> = 0.0916, wR <sub>2</sub> = 0.1618	R <sub>1</sub> = 0.0905, wR <sub>2</sub> = 0.1424

$$^a R_1 = \frac{\sum \|F_o\| - |F_c|}{\sum F_o}, wR_2 = \left\{ \frac{\sum [w(F_o^2 - F_c^2)^2]}{\sum [w(F_o^2)]} \right\}^{1/2}$$

down to room temperature. Green block crystals of **1** along with an amorphous light green impurity were filtered from the colorless mother liquor, washed with distilled water and air-dried at room temperature. The crystals were mechanically separated from the powdery green impurity to give a yield of 61% (based on Cu) and were stable in air and insoluble in water and common organic solvents. IR (KBr, cm<sup>-1</sup>):  $\tilde{\nu}$  = 1583 (m), 1518 (m), 1426 (m), 1088 (m), 968 (m), 912 (m), 785 (m), 716 (m), 525 (m). Elemental anal. Calcd for C<sub>84</sub>H<sub>60</sub>Cl<sub>2</sub>Cu<sub>4</sub>N<sub>14</sub>O<sub>64</sub>P<sub>2</sub>W<sub>18</sub>: C, 16.86; H, 1.01; N, 3.28; P, 1.03; Cl, 1.18; Cu, 4.25; W, 55.28. Found: C, 16.95; H, 1.12; N, 3.42; P, 0.98; Cl, 1.05; Cu, 4.38; W, 58.47.

**Synthesis of [Cu<sub>7</sub>(Phen)<sub>7</sub>(H<sub>2</sub>O)<sub>4</sub>Cl<sub>8</sub>][P<sub>2</sub>W<sub>18</sub>O<sub>62</sub>]·6H<sub>2</sub>O (**2**).** A mixture of LiCl (0.584 g, 13.777 mmol), CuCl<sub>2</sub>·6H<sub>2</sub>O (0.25 g, 1.031 mmol), Na<sub>12</sub>[α-P<sub>2</sub>W<sub>15</sub>O<sub>56</sub>]·18H<sub>2</sub>O (0.5 g, 0.116 mmol), Phen (0.1 g, 0.504) and H<sub>2</sub>O (9 mL, 500 mmol) was stirred for 30 min in air until it was homogeneous, and then transferred and sealed in a 20 mL Teflon-lined stainless steel container. After being heated to 160 °C under autogenous pressure for 5 days, the bomb was cooled down to room temperature. Green block crystals of **2** along with an amorphous green impurity were filtered from the colorless mother liquor, washed with distilled water and air-dried at room temperature. The crystals were mechanically separated from the powdery green impurity to give a yield of 68% (based on Cu) and were stable in air and insoluble in water and common organic solvents. IR (KBr, cm<sup>-1</sup>):  $\tilde{\nu}$  = 3058 (m), 1581 (m), 1516 (m), 1425 (m), 1089 (m), 955 (m), 914 (m), 786 (m), 715 (m), 562 (m). Elemental anal. Calcd for C<sub>84</sub>H<sub>76</sub>Cl<sub>8</sub>Cu<sub>7</sub>N<sub>14</sub>O<sub>72</sub>P<sub>2</sub>W<sub>18</sub>: C, 15.44; H, 1.17; N, 3.00; P, 0.95; Cl, 4.34; Cu, 6.81; W, 50.65. Found: C, 15.67; H, 1.29; N, 3.18; P, 0.89; Cl, 4.45; Cu, 6.98; W, 50.979.

**X-ray Crystallography.** The reflection intensities of **1** and **2** were collected on a SMART CCD diffractometer equipped with graphite monochromatic Mo Kα radiation (λ = 0.71073 Å) at 293 K. The linear absorption coefficients, scattering factors for the atoms, and anomalous dispersion corrections were taken from *International Tables for X-ray Crystallography*. The structures were solved by the direct method and refined by the full-matrix least squares method on F<sup>2</sup> using the SHELXTL crystallographic software package. Hydrogen atoms on the Phen ligands were placed on calculated positions and included in the refinement riding on their respective parent atoms. Anisotropic thermal parameters were used to refine all non-hydrogen atoms except for part of oxygen and carbon atoms. Those hydrogen atoms attached to lattice water molecules were not located. CCDC 716000 and 716001 contain the supplementary crystallographic data for this paper. These data can be obtained free of charge at <http://www.ccdc.cam.ac.uk/conts/retrieving.html> (or from the Cambridge Crystallographic Data Centre, 12, Union Road, Cambridge CB2 1EZ, U.K.; fax, +44-1223/336-033; e-mail, [deposit@ccdc.cam.ac.uk](mailto:deposit@ccdc.cam.ac.uk)). The crystal data and structure refinement results of **1** and **2** are summarized in Table 1. Selected bond lengths and bond angles for **1** and **2** are provided in Tables S1 and S2 in the Supporting Information.

## Results and Discussion

**Synthesis.** In these experiments, **1** and **2** contain plenary [P<sub>2</sub>W<sub>18</sub>O<sub>62</sub>]<sup>6-</sup> polyoxoanions, although the reaction was carried

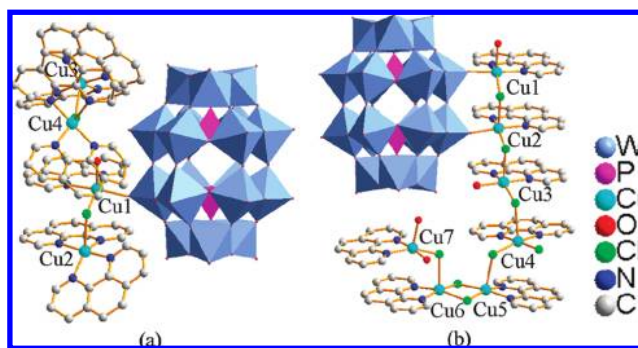
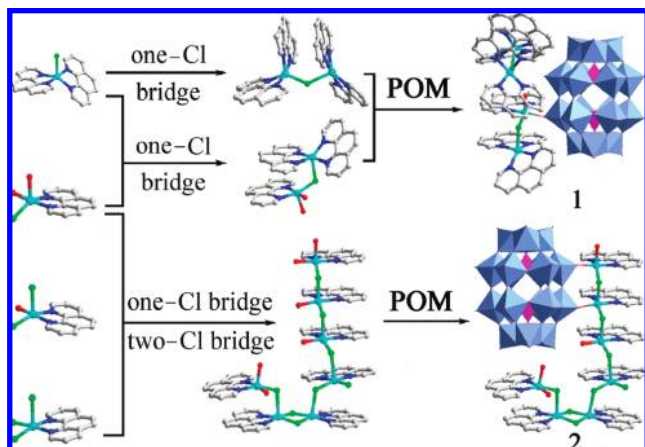


**Figure 1.** The molecular structural units of **1** (a) and **2** (b) with the selected atomic labeling scheme. The water molecules of crystallization and hydrogen atoms are omitted for clarity.

out by using vacant polyoxoanion as the starting material. The lacunary polyoxoanions [α-P<sub>2</sub>W<sub>15</sub>O<sub>56</sub>]<sup>12-</sup> and [H<sub>2</sub>P<sub>2</sub>W<sub>12</sub>O<sub>48</sub>]<sup>12-</sup> respectively transformed the saturated Dawson-type polyoxoanions [P<sub>2</sub>W<sub>18</sub>O<sub>62</sub>]<sup>6-</sup> and resulted in two new products with different structure features. Many experimental results have proved that vacant Dawson-type polyoxoanions can be transformed saturated polyoxoanions under acidic conditions.<sup>12</sup> It is worth noting that **1** and **2** cannot be synthesized by [P<sub>2</sub>W<sub>18</sub>O<sub>62</sub>]<sup>6-</sup> precursors under hydrothermal conditions. Furthermore, the presence of LiCl is necessary for the formation of compounds **1** and **2**. When the reactions were performed in the absence of LiCl, nothing could be obtained except for some unknown green powder. When we replaced LiCl with an equal amount of NaCl, KCl or CsCl in the reaction systems, **1** and **2** could not be obtained.

**Description of the Crystal Structures.** The crystal structure analyses reveal that compounds **1** and **2** belong to the triclinic and monoclinic crystal systems, respectively. They contain a Dawson-type polyanion and different types of copper-phenanthroline complexes of variable nuclearities (Figure 1). The main structural feature of these two compounds is the presence in different copper-phenanthroline complex moieties which compose new multinuclear copper-Phen complexes linked by Cu-Cl bond (Scheme 1). The [P<sub>2</sub>W<sub>18</sub>O<sub>62</sub>]<sup>6-</sup> anion is the inorganic building block in compounds **1** and **2**, and all of the bond lengths and angles are within the normal ranges and consistent with those described in the literature.<sup>13</sup> The valence sum calculations of compounds **1** and **2** show that all of the W atoms are in the +VI oxidation state and the Cu atoms are in the +II oxidation state.<sup>14</sup> Moreover, EPR spectra (Figures S3

Scheme 1



and S4 in the Supporting Information) of **1** and **2** also confirm that Cu atoms are in the +II oxidation state.

**Crystal Structure of Compound 1.** The structure of **1** is solved in the monoclinic chiral space group  $P2_1$ , and it contains one  $[P_2W_{18}O_{62}]^{6-}$  anion covalently linked to one Cl-bridged dinuclear copper complex  $[Cu_2(Phen)_3(H_2O)Cl]^{3+}$ , one dinuclear  $[Cu_2(Phen)_4Cl]^{3+}$  cation and one lattice water molecule (Figure 1a). The two different dinuclear copper fragments with Cl and Phen as bridging and peripheral ligands, respectively, are present in the crystal structure. The  $[Cu_2(Phen)_3(H_2O)Cl]^{3+}$  cation links POM by a terminal oxygen atom from  $[P_2W_{18}O_{62}]^{6-}$ , and the  $[Cu_2(Phen)_4Cl]^{3+}$  cation appears as an isolated dimeric cationic species. They contain four independent copper centers in which all of Cu could be described as having a “4 + 1” coordination geometry (Figure S7 in the Supporting Information). The Cu(1) atom is coordinated by one oxygen atom from  $[P_2W_{18}O_{62}]^{6-}$ , two nitrogen atoms of a Phen ligand, one Cl atom and one solvent  $H_2O$  molecule (Figure S7a in the Supporting Information). For Cu(2), Cu(3) and Cu(4), besides four nitrogen atoms from two Phen ligands, a chlorine atom is bonded to it, respectively (Figure S7f in the Supporting Information). The ranges of bond distances and angles around the Cu ions are 2.30–2.62 Å for Cu–Cl, 1.96–2.19 Å for Cu–N, 2.01–2.12 Å for Cu–O, and 78.9–83.9° for N–Cu–N. An unusual feature of **1** is that the components are closely packed along the  $2_1$  screw axis to generate chiral helical chains (as shown in Figure 2). To the best of our knowledge, compound **1** represents a new model to assemble the chiral POM-based compounds from achiral building blocks by supramolecular arrangements. However, the flack parameter (0.5) indicates that **1** is just a twin crystal containing two enantiomers simultaneously with the content of ca. 50 and 50%, respectively.<sup>15</sup> In the packing arrangement, all of the molecular structural units are stably stacked together into 3-D supramolecular framework via  $\pi$ – $\pi$  and electrostatic interactions.

**Crystal Structure of Compound 2.** Single crystal X-ray diffraction analysis reveals that compound **2** consists of one  $[P_2W_{18}O_{62}]^{6-}$  anion, one heptanuclear  $[Cu_7(phen)_7(H_2O)_4Cl_8]^{6+}$  cation and six  $H_2O$  molecules (Figure 1b). More particularly, the unusual heptanuclear copper chain  $[Cu_7(phen)_7(H_2O)_4Cl_8]^{6+}$  is formed by means of a Cu–Cl bond, Cu(5) and Cu(6) are linked by a two-Cl bridge and others by a one-Cl bridge. In this heptanuclear copper chain, each Cu atom is 5-coordinate and shows distorted square pyramidal geometry (Figure S7 in the Supporting Information). The Cu(1) atom is coordinated by one oxygen atom from  $[P_2W_{18}O_{62}]^{6-}$ , two nitrogen atoms from

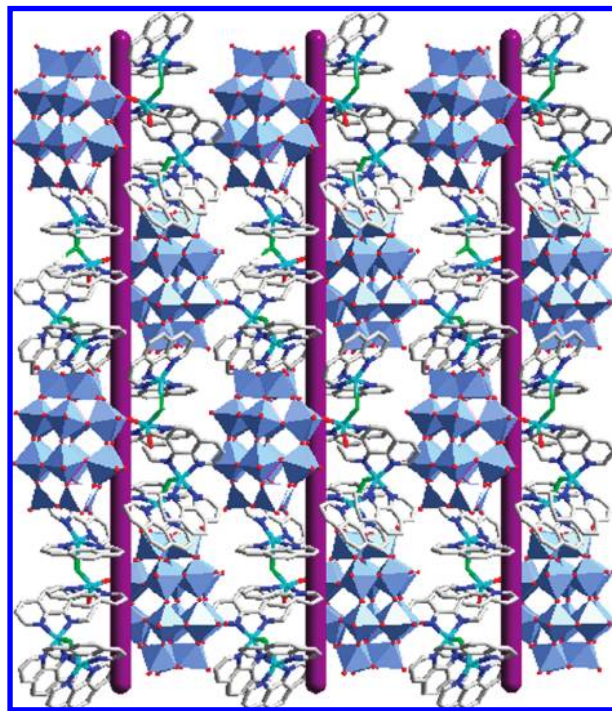


**Figure 2.** The packing arrangement of **1**. H atoms and lattice water molecules have been omitted for clarity.

Phen ligand, one Cl atom and one  $H_2O$  molecule (Figure S7a in the Supporting Information). Cu(2) atom is coordinated by a terminal oxygen atom of  $[P_2W_{18}O_{62}]^{6-}$  anion, two nitrogen atoms of Phen ligand and two Cl atoms (Figure S7b in the Supporting Information). Cu(3) atom is coordinated by two nitrogen atoms from Phen ligand, two Cl atoms and one  $H_2O$  molecule (Figure S7c in the Supporting Information). Cu(4), Cu(5) and Cu(6) are coordinated by two Phen nitrogen atoms and three Cl atoms, respectively (Figure S7d in the Supporting Information). Cu(7) is coordinated by two nitrogen atoms of Phen ligand, one Cl atom and two  $H_2O$  molecules (figure S7e). The bond distances around the Cu(II) are 2.24–2.64 Å (Cu–Cl), 1.98–2.04 Å (Cu–N) and 1.94–2.19 Å (Cu–O), the N–Cu–N angles are 80.6–82.9°, and the Cl–Cu–Cl angles are 98.9–104.1°. The coordinated cation  $[Cu_7(phen)_7(H_2O)_4Cl_8]^{6+}$  connects with  $[P_2W_{18}O_{62}]^{6-}$  through two terminal oxo groups of tungsten sites with Cu–O distances which are 1.95 (Cu1–O) and 1.99 Å (Cu2–O), respectively. Each  $[Cu_7(Phen)_7(H_2O)_4Cl_8][P_2W_{18}O_{62}]$  molecule is further stacked by aromatic  $\pi$ – $\pi$  stacking interaction of Phen groups (separation 3.57–3.78 Å) to form a 3D supramolecular network (Figure 3).

In a comparative analysis on structures of compounds **1** and **2**, all of the Cu centers display “4 + 1” coordination geometry. Such coordination geometry is consistent with the fact that the  $Cu^{II}$  ion with a  $d^9$  configuration tends to have a “4 + 1” coordination geometry because of a strong Jahn–Teller distortion effect. Otherwise, the organic component plays an important role in determining the packing arrangements of organic–inorganic assemblies, in contrast to the inorganic component directing the ordered assembly of the organic moiety. The mechanism of the formation of different assemblies is not yet understood. However, the successful synthesis of **1** and **2** shows that the appropriate combination of materials, size and ratio of anion and cation, and hydrothermal synthetic conditions can lead to the formation of POM-based complexes with different geometrical and structural characteristics.

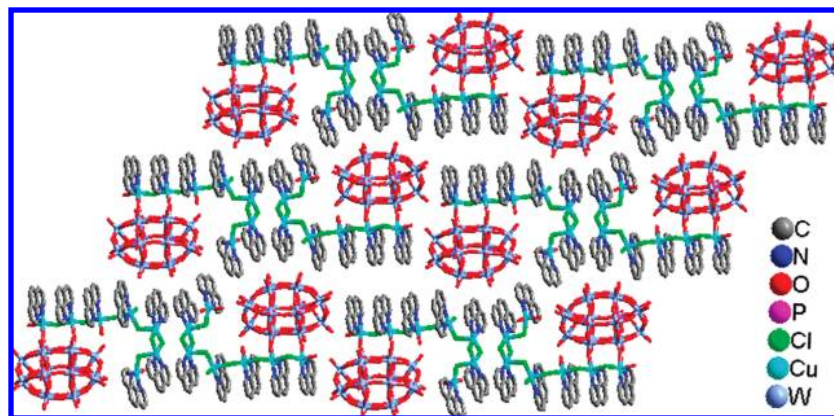


**Figure 3.** The packing arrangement of **2**. H atoms and lattice water molecules have been omitted for clarity.

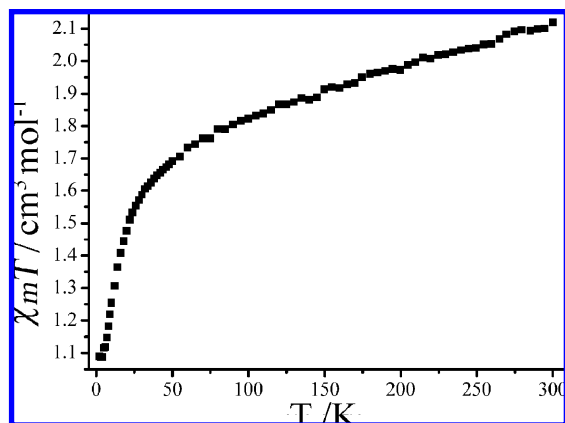


**Figure 4.** Temperature dependence of  $\chi_m T$  for **1** at 1000 Oe.

**Thermogravimetric Analysis.** Thermogravimetric (TG) measurements of **1** and **2** were investigated and also supported their chemical composition (see Figures S5 and S6 in the Supporting Information). In compound **1**, a total weight loss of 21.95% is accordant with the calculated value of 21.68% in the range of 27–600 °C, ascribed to the release of two water and seven Phen molecules. The TG curve of **2** exhibits a two step continuing weight loss of 22.39% in the temperature range 27–600 °C, which agrees with the calculated value of 22.07%. The first weight loss is 3.01% below 190 °C, which corresponds to the loss of all lattice and coordinated water molecules (calcd 2.76%). The second weight loss is 19.38% at 190–600 °C, assigned to the decomposition of Phen ligands (calcd 19.31%). The samples of **1** and **2** do not lose weight at temperatures higher than 600 °C.

**Magnetic Susceptibility.** The solid-state magnetic behaviors of **1** and **2** have been investigated at 1000 Oe in the temperature range of 2–300 K. For **1**, the  $\chi_m T$  value at 300 K of 2.12 cm<sup>3</sup> K mol<sup>-1</sup> is well below the expected value for two noninteracting spin Cu<sup>II</sup> ( $S = 1/2$ ) ions with  $g = 2.0$  (2.12 cm<sup>3</sup> K mol<sup>-1</sup>; Figure 4). With decreasing temperature, the  $\chi_m T$  value decreases to a minimum of 1.09 cm<sup>3</sup> K mol<sup>-1</sup> at 2 K. This behavior is indicative of the presence of antiferromagnetic spin exchange interactions between the Cu<sup>II</sup> centers. The  $1/\chi_m$  versus  $T$  plot of **1** is in correspondence with Curie–Weiss law in the range of 2–300 K with  $C = 2.12$  cm<sup>3</sup> K mol<sup>-1</sup> and  $\theta = -11.26$  K (Figure S10 in the Supporting Information).

For **2**, the  $\chi_m T$  value at 300 K is 2.80 cm<sup>3</sup> K mol<sup>-1</sup>, smaller than the expected value (3.58 cm<sup>3</sup> K mol<sup>-1</sup>) of seven isolated spin only Cu<sup>II</sup> ions ( $S = 1/2$ ,  $g = 2.0$ ; Figure 5). The product

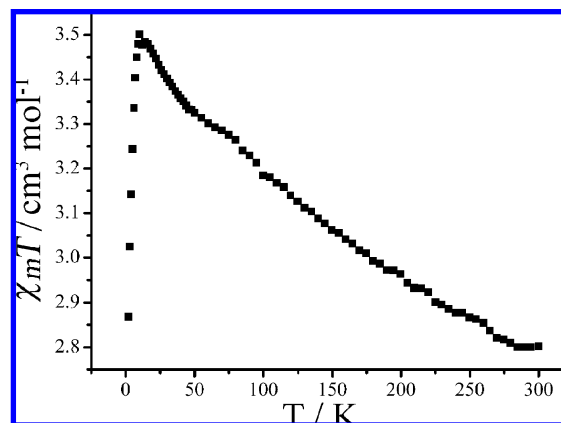


**Figure 5.** Temperature dependence of  $\chi_m T$  for **2** at 1000 Oe.

$\chi_m T$  increases on cooling to a maximum 3.50 cm<sup>3</sup> K mol<sup>-1</sup> at 10 K, which indicates the presence of ferromagnetic exchange coupling. Subsequently, the curve drops abruptly below 10 K, which may be caused by the zero-field splitting contributions or saturation effects are likely to influence the data in this temperature range. The measured data of **2** was fitted by using the Curie–Weiss equation  $\chi_m = C_m/(T - \theta)$  in the range of 2–300 K with  $C = 2.98$  cm<sup>3</sup> K mol<sup>-1</sup> and  $\theta = 4.74$  K (Figure S11 in the Supporting Information).

Although each Cu(II) is linked by Cl atoms, compounds **1** and **2** display ferromagnetic and antiferromagnetic exchange coupling, respectively. The different Cu–Cl–Cu magnetic behaviors maybe depend on the angle. In **1**, the Cu–Cl–Cu angle (108.6–130.2°) is close to 180° and could give antiferromagnetic coupling. However, the Cu–Cl–Cu angle (92.6–117.1°) of **2** is close to 90° and could give ferromagnetic coupling. Especially, Cu–Cl–Cu (92.6°) angles linked by a two-Cl bridge could result in larger interchain exchange with ferromagnetic coupling.<sup>16</sup> It is similar to those obtained for Cu–O–Cu coupling.<sup>6b,17</sup>

**Electrochemical Properties of 2-CPE.** In order to investigate the electrochemical behavior of **2**, **2** has been used as a modifier to fabricate chemically modified carbon paste electrodes (2-CPE) due to their high thermal stability and low solubility in water and common organic solvents. The cyclic voltammograms for 2-CPE in 1 M H<sub>2</sub>SO<sub>4</sub> aqueous solution were recorded in the potential range of +600 to –700 mV (scan rate: 80 mV·s<sup>-1</sup>, Figure 6). The reduction peak I and its oxidation counterpart I' correspond to the redox processes of the Cu<sup>II</sup> centers. Three reversible redox waves are obtained with midpoint potentials

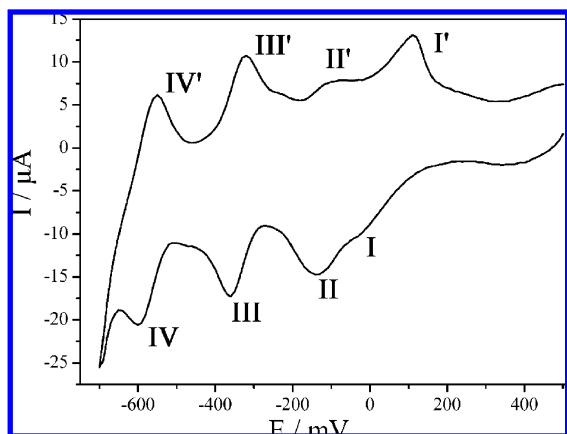


**Figure 6.** Cyclic voltammograms of the 2-CPE in the 1 M H<sub>2</sub>SO<sub>4</sub> solution at scan rates of mV·s<sup>-1</sup>.

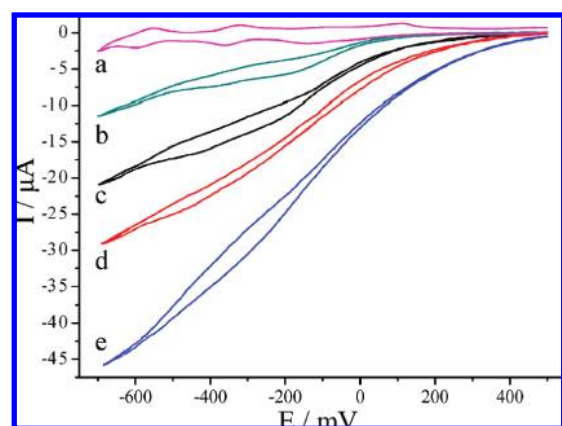


**Figure 7.** Cyclic voltammograms of 2-CPE in 1 M H<sub>2</sub>SO<sub>4</sub> solution containing (a) 0 mM, (b) 2.5 mM, (c) 5 mM, (d) 10 mM, and (e) 20 mM NaNO<sub>2</sub>. Scan rate: 100 mV·s<sup>-1</sup>.

( $E_{\text{mid}}$ ) of  $-120$  (II–II'),  $-340$  (III–III'), and  $-575$  (IV–IV') mV, where  $E_{\text{mid}} = (E_{\text{pc}} + E_{\text{pa}})/2$ ;  $E_{\text{pc}}$  and  $E_{\text{pa}}$  are the cathodic and anodic peak-potentials, respectively. The redox peaks, II–II', III–III' and IV–IV' correspond to three consecutive two-electron processes of the W centers.<sup>18</sup> The peak currents were proportional to the scan rate up to  $250$  mV·s<sup>-1</sup>, indicating that the redox process of 2-CPE is surface-controlled (Figure S12 in the Supporting Information).<sup>19</sup>

Catalytic reduction of NO<sub>x</sub> species, especially of nitrite reduced by POMs, has become a classical test for their electrocatalytic abilities. And the electrocatalytic reduction of nitrate remains a challenge in the NO<sub>x</sub> series because a complete process requires several electrons. Therefore, electrocatalytic reduction of NO<sub>2</sub><sup>-</sup> by the 2-CPE constitutes a further step in the search for its electrocatalytic activity. We found that 2-CPE displays good electrocatalytic activity toward the reduction of nitrite. On addition of NO<sub>2</sub><sup>-</sup>, all the reduction peak currents increase, and the corresponding oxidation peak currents decrease dramatically, which indicate that the four reduced species all show electrocatalytic activity toward the reduction of nitrite (Figure 7). Notice that because Cu<sup>II</sup> retains its catalytic properties, it is possible to accumulate Cu<sup>II</sup> active centers and also fabricate highly reduced species with the electrons accumulated in the reduced tungstophosphate.<sup>20</sup> Moreover, 2-CPE is very stable. The voltammetric behavior of the 2-CPE remains almost unchanged after hundreds of cycles at a scan rate of  $100$  mV·s<sup>-1</sup>. After 2-CPE was stored at room temperature for 1

month, the peak current decreased only slightly and could be renewed by squeezing a little carbon paste out of the tube. This is especially useful for electrocatalytic studies, since the catalytic activity is known to decrease when the electrode is fouled.<sup>21</sup> Thus, 2-CPE could be an ideal electrode material for investigating electrocatalytic properties.

## Conclusions

In this paper, by designing the usage of different POM precursors and copper–Phen complexes, two organic–inorganic hybrid compounds **1** and **2** based on [P<sub>2</sub>W<sub>18</sub>O<sub>62</sub>]<sup>6-</sup> have been synthesized under hydrothermal conditions. Interestingly, the different copper–Phen complex moieties compose new copper–Phen complexes, which are of different nuclearities, linked by a Cu–Cl bond in these two compounds. The Cu–Cl–Cu angles of binuclear and heptanuclear copper–Phen complexes are close to 180° and 90°, respectively. This difference induces that **1** and **2** exhibit antiferromagnetic and ferromagnetic spin exchange interactions between the Cu<sup>II</sup> centers, respectively. The high thermal stability and extremely low solubility in various solvents as well as the POM-enriched character suggest that **1** and **2** could be an ideal hybrid material for electrocatalysis. The 2-CPE displays a good electrocatalytic activity toward the reduction of nitrite. This work reveals that appropriate combination of materials, size and ratio of anion and cation, and hydrothermal synthetic conditions can lead to the formation of POM-based complexes with different structural and functional characteristics.

**Acknowledgment.** This work was supported by NSFC (Grant NO. 20871027), Program for New Century Excellent Talents in University (NCET-07-0169), and Program for Changjiang Scholars and Innovative Research Team in University.

**Supporting Information Available:** Tables of selected bond lengths and angles for compounds **1** and **2**; IR spectra, TG spectra, EPR spectra, and structural, magnetic, and electrochemical figures for compounds **1** and **2**; and crystallographic information files. This material is available free of charge via the Internet at <http://pubs.acs.org>.

## References

- (1) (a) Hagraman, P. J.; Hagraman, K.; Zubieta, J. *Angew. Chem., Int. Ed.* **1999**, *38*, 2638–2684. (b) Chesnut, D. J.; Hagraman, D.; Zapf, P. J.; Hammond, R. P.; LaDuca, R., Jr.; Haushalter, R. C.; Zubieta, J. *Coord. Chem. Rev.* **1999**, *190–192*, 737–769. (c) Hagraman, P. J.; Finn, R. C.; Zubieta, J. *Solid State Sci.* **2001**, *3*, 745–774. (d) Gouzerh, P.; Proust, A. *Chem. Rev.* **1998**, *98*, 77–111.
- (2) (a) Xie, L.-H.; Liu, S.-X.; Gao, B.; Zhang, C.-D.; Sun, C.-Y.; Li, D.-H.; Su, Z.-M. *Chem. Commun.* **2005**, 5023–5025. (b) Dolbecq, A.; Mialane, P.; Lisnard, L.; Marrot, J.; Sécheresse, F. *Chem.–Eur. J.* **2003**, *9*, 2914–2920. (c) Zapf, P. J.; Warren, C. J.; Haushalter, R. C.; Zubieta, J. *Chem. Commun.* **1997**, 1543–1544. (d) Yuan, M.; Li, Y.-G.; Wang, E.-B.; Tian, C.-G.; Wang, L.; Hu, C.-W. *Inorg. Chem.* **2003**, *42*, 3670–3676.
- (3) (a) Férey, G. *Chem. Mater.* **2001**, *13*, 3084–3098. (b) Bunkholder, E.; Golub, V.; O'Connor, C. J.; Zubieta, J. *Inorg. Chem.* **2004**, *43*, 7014–7029. (c) Zhang, C.-D.; Liu, S.-X.; Gao, B.; Sun, C.-Y.; Xie, L.-H.; Yu, M.; Peng, J. *Polyhedron* **2007**, *26*, 1514–1522.
- (4) (a) Sha, J.-Q.; Peng, J.; Lan, Y.-Q.; Su, Z.-M.; Pang, H.-J.; Tian, A.-X.; Zhang, P.-P.; Zhu, M. *Inorg. Chem.* **2008**, *47*, 5145–5153. (b) Sun, C.-Y.; Liu, S.-X.; Liang, D.-D.; Shao, K.-Z.; Ren, Y.-H.; Su, Z.-M. *J. Am. Chem. Soc.* **2009**, *131*, 1883–1888. (c) Kögerler, P.; Cronion, L. *Angew. Chem., Int. Ed.* **2005**, *44*, 844–846.
- (5) Burrows, A. D.; Chan, C. W.; Chowdhry, M. M.; McGrady, J. E.; Minos, D. M. P. *Chem. Soc. Rev.* **1995**, *24*, 329–339.
- (6) (a) Ushak, S.; Spodine, E.; Fur, E. L.; Venegas-Yazigi, D.; Pivan, J.-Y.; Schnelle, W.; Cardoso-Gil, R.; Kniep, R. *Inorg. Chem.* **2006**, *45*, 5393–5399. (b) Ghosh, A. K.; Ghoshal, D.; Ribas, J.; Mostafa, G.; Chaudhuri, N. R. *Cryst. Growth Des.* **2006**, *6*, 36–39. (c) Wang, S.-T.; Wang, E.-B.; Hou, Y.; Li, Y.-G.; Yuan, M.; Hu, N.-H. *Inorg. Chim. Acta* **2003**, *349*, 123–127.

- (7) Shivaiah, V.; Chatterjee, T.; Srinivasu, K.; Das, S. K. *Eur. J. Inorg. Chem.* **2007**, 231–234.
- (8) (a) Reinoso, S.; Vitoria, P.; Felices, L. S.; Lezama, L.; Gutiérrez-Zorrilla, J. M. *Chem.—Eur. J.* **2005**, *11*, 1538–1548. (b) Reinoso, S.; Vitoria, P.; Felices, L. S.; Lezama, L.; Gutiérrez-Zorrilla, J. M. *Inorg. Chem.* **2006**, *45*, 108–118. (c) Reinoso, S.; Vitoria, P.; Gutiérrez-Zorrilla, J. M.; Lezama, L.; Madariaga, J. M.; Felices, L. S.; Iturrospe, A. *Inorg. Chem.* **2007**, *46*, 4010–4021.
- (9) (a) Bond, M. R.; Willett, R. D.; Rubenacker, G. V. *Inorg. Chem.* **1990**, *29*, 2713–2720. (b) Chesnut, D. J.; Kusnetzow, A.; Brige, R. R.; Zubieta, J. *Inorg. Chem.* **1999**, *38*, 2663–2671.
- (10) (a) Ayllón, J. A.; Santos, I. C.; Henriques, R. T.; Almeida, M.; Alcácer, L.; Duarte, M. T. *Inorg. Chem.* **1996**, *35*, 168–172. (b) Rojas, D.; Garcia, A. M.; Vega, A.; Moreno, Y.; Venegas-Yazigi, D.; Garland, M. T.; Manzur, J. *Inorg. Chem.* **2004**, *43*, 6324–6330.
- (11) Contant, R. *Inorg. Synth.* **1990**, *27*, 104–111.
- (12) (a) Zimmermann, M.; Belai, N.; Butcher, R. J.; Pope, M. T.; Chubarova, E. V.; Dickman, M. H.; Kortz, U. *Inorg. Chem.* **2007**, *46*, 1737–1740. (b) Wang, E.-B.; Hu, C.-W.; Xu, L. *Introduction of Polyacid Chemistry*; Chemical Industry Press: Beijing, 1998.
- (13) (a) Niu, J.-Y.; Guo, D.-J.; Zhao, J.-W.; Wang, J.-P. *New J. Chem.* **2004**, *28*, 980–987. (b) Lu, Y.; Xu, Y.; Li, Y.-G.; Wang, E.-B.; Xu, X.-X.; Ma, Y. *Inorg. Chem.* **2006**, *45*, 2005–2060. (c) Tian, A.-X.; Ying, J.; Peng, J.; Sha, J.-Q.; Han, Z.-G.; Ma, J.-F.; Su, Z.-M.; Hu, N.-H.; Jia, H.-Q. *Inorg. Chem.* **2008**, *47*, 3274–3283.
- (14) (a) Brown, I. D.; Altermatt, D. *Acta Crystallogr.* **1987**, *B41*, 244–246. (b) Brese, N. E.; O’Keeffe, M. *Acta Crystallogr.* **1991**, *B47*, 192–197.
- (15) (a) Flack, H. D.; Bernardinelli, G. *Acta Crystallogr., Sect. A* **1999**, *55*, 908–915. (b) Chen, W.-L.; Li, Y.-G.; Wang, Y.-H.; Wang, E.-B. *Eur. J. Inorg. Chem.* **2007**, 2216–2220.
- (16) (a) Estes, W. E.; Gavel, D. P.; Hatfield, W. E.; Hodgson, D. J. *Inorg. Chem.* **1978**, *17*, 1415–1421. (b) Rodríguez, M.; Llobet, A.; Corbella, M.; Martell, A. E.; Reibenspies, J. *Inorg. Chem.* **1999**, *38*, 2328–2334.
- (17) Kahn, O. *Molecular Magnetism*; VCH: New York, 1993.
- (18) (a) Sadakane, M.; Steckhan, E. *Chem. Rev.* **1998**, *98*, 219–237. (b) McCormac, T.; Fabre, B.; Bidan, G. *J. Electroanal. Chem.* **1997**, *425*, 49–54.
- (19) Cheng, L.; Zhang, X.-M.; Xi, X.-D.; Liu, B.-F.; Dong, S.-J. *J. Electroanal. Chem.* **1996**, *407*, 97–103.
- (20) Keita, B.; Mbomekalle, I.-M.; Nadjo, L. *Electrochem. Commun.* **2003**, *5*, 830–837.
- (21) Zhao, X.-Y.; Liang, D.-D.; Liu, S.-X.; Sun, C.-Y.; Cao, R.-G.; Gao, C.-Y.; Ren, Y.-H.; Su, Z.-M. *Inorg. Chem.* **2008**, *47*, 7133–7138.

CG900391Q